EXTENSION OF TEST TIME IN LUDWIEG TUNNELS

Jack Hillyer, Luke Doherty, Chris Hambidge, Matthew McGilvray

University of Oxford
Department of Engineering Science
Parks Rd, Oxford

ABSTRACT

Two new, longer duration, modes of operation for Ludwieg Tunnels have been implemented in the Oxford High Density Tunnel (HDT): Extended Ludwieg Mode (ELM) and Plenum Augmented Ludwieg Mode (PALM). In standard Ludwieg Tunnel operation, the duration of the steady test time is limited by the return of the rarefaction wave to the facility nozzle throat. Operation in ELM extends the rarefaction wave such that the tail is generated as the head returns and results in a steady decrease in supply pressure. PALM takes advantage of the dual-throat arrangement of the HDT, which features a plenum region between the facility barrel and the nozzle throat, and tailors plug valve opening to produce a steady supply pressure to the facility nozzle at the expense of total pressure capability. This paper describes the theory of operation of these new modes, their implementation in the existing Oxford High Density Tunnel and presents transient quasi-1D numerical simulations confirming their principles of operation. It then presents experimental results from initial testing of the HDT in the new modes. These results demonstrate a successful implementation of ELM, producing a test flow that is over fifteen times longer, but of comparable steadiness to a Mach 7 Ludwieg Mode plateau in the Oxford HDT. PALM was implemented with partial success, resulting in a test flow that is both ten times the duration of, and significantly steadier (for supply pressure and unit Reynolds number), than a Ludwieg Mode plateau. Thus, the implementation of ELM and PALM significantly expand the capability of the facility to investigate long duration flow phenomena.

Index Terms— Ground testing, Low enthalpy, Ludwieg Tunnel, Test time, ELM, PALM

1. INTRODUCTION

Extensive ground testing is used during the design of a hypersonic vehicle for two key purposes: 1) as a cheap, low-risk alternative to flight tests for determining vehicle characteristics and behaviour [1] and 2) in support of CFD studies via provision of validation data and investigation of un-modelled phenomena [2, 3, 4]. However, the hypersonic flight regime is inherently complex and a single wind tunnel is not capable of replicating all of the effects of hypersonic flight simultaneously. For this reason, ground testing is often performed in an array of hypersonic facilities, each with their own limitations [5]. One limitation common to all hypersonic facilities is their intermittent operation: test times are limited to minutes at most and are typically inversely proportional to flow enthalpy [6]. Full scale, continuous hypersonic wind tunnels are not feasible due to high structural and thermal loads and total power required (order of GigaWatts) [7].

Given that there are limited continuous hypersonic flow facilities, there is significant importance on the length of test time, which must be greater than the flow establishment time of quantities of interest. Additionally, increased test time broadens the range of experiments that can be performed, allowing for better vehicle characterisation. The steadiness of the test flow is determined by the magnitude of the terms of the total derivative of any flow property λ, given in Eqn. (1). The total derivative can be broken down into a local term, $\frac{\partial \lambda}{\partial t}$, and a sum of convective terms. A test flow is said to be steady during a chosen interval (i.e. the test time) if the local term is zero, and quasi-steady if the local term is non-zero but much smaller than the convective terms. Further information on quasi-steady flows and associated data analysis techniques are given in [8, 9].

$$\frac{D\lambda}{Dt} = \frac{\partial \lambda}{\partial t} + U\frac{\partial \lambda}{\partial x} + V\frac{\partial \lambda}{\partial y} + W\frac{\partial \lambda}{\partial z} \tag{1}$$

The facilities with the longest test times available are blowdown facilities, which can produce flows matching flight Reynolds number for test times on the order of seconds or minutes. However, these facilities are costly to run, require significant infrastructure and cannot reproduce higher flight enthalpies. Impulse tunnels, which operate by instantaneously releasing high energy gas to produce hypersonic flows, avoid the containment issues that affect the design of continuous hypersonic flow facilities by only operating for short periods of time. High enthalpy impulse facilities are able to replicate the higher flight enthalpies, but only produce test flows that are of extremely short duration (from tens of microseconds to tens of milliseconds). Additionally, the rapid expansion of a high-temperature equilibrium gas can lead to frozen species present in the test flow that aren't

representative of flight. Low enthalpy impulse tunnels generally produce cold perfect gas flows, allowing for simulation of flight Reynolds number and Mach number, but not high temperature gas effects. Fig. 1 provides an overview of the capabilities of different hypersonic facilities in terms of simulated flight velocity and test time.

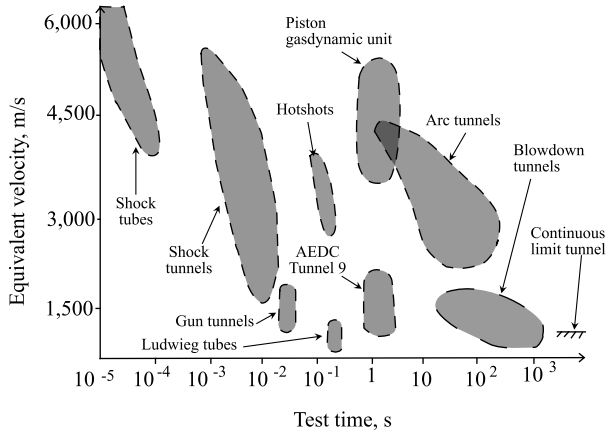

Fig. 1: Equivalent velocity vs test times for hypersonic facilities. Adapted from [6]

One common type of low enthalpy impulse facility is a Ludwieg Tunnel, which generally consists of a barrel filled with high pressure gas connected to a nozzle via a fast-acting valve or a diaphragm. Fig. 2 shows a schematic diagram and distance-time (x-t) wave plot for a Ludwieg tunnel operating in Ludwieg Mode (LM). In LM, flow is initiated by rapidly opening a valve or bursting a diaphragm, resulting in a rarefaction wave travelling upstream. Steady supply conditions to the facility nozzle are attained until the rarefaction wave returns to the nozzle throat, resulting in a decrease in supply pressure. Unless the test is then terminated, the rarefaction wave reflects, travels back upstream and the process repeats. This results in a classic Ludwieg trace consisting of several steady flow plateaus, shown schematically in Fig. 2. The length of each plateau, t_{wr}, is given by the length of time it takes for the rarefaction wave to return to the valve/diaphragm:

$$t_{wr} \approx \frac{2L}{a} \tag{2}$$

Where L is the length of the facility barrel and a is the speed of sound of the gas in the barrel. For the Oxford High Density Tunnel, t_{wr} varies between 35-50 ms [10].

Traditionally, extension of test times in Ludwieg tunnels is achieved via an increase in facility length [11]. *Jones et al* [12] proposed two new modes of operation for Ludwieg Tunnels aimed at extending the test time: Extended Ludwieg Mode (ELM) and Plenum Augmented Ludwieg Mode (PALM). In ELM, the opening time of the valve is increased

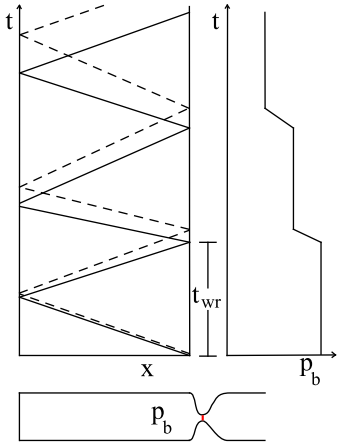

Fig. 2: x-t and p-t diagrams of a Ludwieg tunnel operating in Ludwieg Mode. The red line in the schematic indicates the location of the fast acting valve or diaphragm

to equal t_{wr}. This extends the rarefaction wave, resulting in a steady decrease in nozzle supply pressure. This sacrifices the steadiness of a LM plateau, but greatly extends the test duration. PALM requires the Ludwieg Tunnel to have a dual-throat arrangement, with a plenum between the barrel and the facility nozzle and the plug valve at the upstream end. The barrel is then operated in ELM and the valve opening is further controlled to balance the head loss decrease across the valve to the drop in barrel pressure. This results in constant supply pressure to the facility nozzle, greatly extending the available steady test time to be comparable to some blowdown facilities (without an increase in size of the Ludwieg tunnel). However, this extension of test time comes at the expense of total pressure and unit Reynolds number capability. If higher unit Reynolds numbers are required, the tunnel must be operated in Ludwieg Mode.

ELM has been successfully demonstrated by both *Jones et al* in the DRA Shock Tunnel (now the Oxford High Density Tunnel), and by *Kimmel et al* [13] at the Air Force Research Laboratory, but to the authors knowledge PALM has never been implemented in a Ludwieg tunnel.

This paper presents experimental results of the implementation of ELM and PALM to extend the test times available in the Oxford High Density Tunnel, a Ludwieg tunnel. This paper is structured as follows: Section 2 discusses the fluid dynamics and required valve opening for each new mode. Section 3 provides an overview of the Oxford High Density Tunnel and how the new modes were implemented in this facility. Section 4 details numerical simulations of the Oxford High Density Tunnel operating in the new modes, and Section 5 discusses the experimental results.

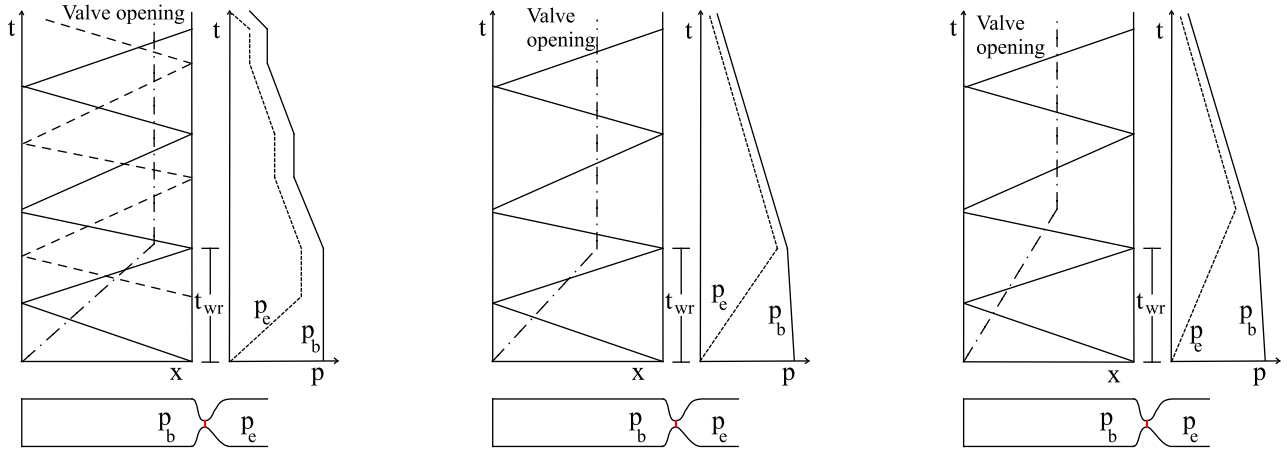

(a) $t_{op} < t_{wr}$ (b) $t_{op} < t_{wr}$ c) $t_{op} > t_{wr}$

Fig. 3: Schematic x-t and p-t diagrams showing the effect of different valve openings on the resultant ELM trace. The red line in the schematics indicates the location of the fast acting valve

2. THEORY OF OPERATION OF NEW MODES

2.1. ELM

This section presents the effect of valve opening time on the achievement of ELM. To achieve ELM, the opening time of the valve, t_{op}, must be greater than or equal to t_{wr}, extending the rarefaction wave such that the tail is generated as the head of the wave returns. Assuming the valve opens fully in time t_{op}, if:

$t_{op} < t_{wr}$: Pseudo-ELM; Fig. 3a attained. The tail of the rarefaction wave will be generated before the head returns. Results in short periods of constant supply pressure.

$t_{op} = t_{wr}$: *Desired* ELM; Fig. 3b attained. Supply pressure trace will be a steady fall passing through the end of each plateau on the LM trace. The $\frac{dp_e}{dt}$ achieved will be dependent on the facility length, with longer lengths resulting in steadier supply pressures.

$t_{op} > t_{wr}$: ELM; Fig. 3c attained. The tail of the rarefaction wave will be generated after the head returns. This results in a steady fall in supply pressure, but the rise time is greater and the peak supply pressure will be lower than *desired* ELM.

The above relations between t_{op} and t_{wr} hold true if the valve only partially opens, though the maximum nozzle supply pressure achieved will be reduced compared with a fully open valve.

2.2. PALM

Implementation of PALM requires the Ludwieg tube to have two features: 1) The facility must have a plenum upstream of the nozzle throat and 2) the facility valve must be designed such that the head loss across it is a function of valve opening. The plenum acts as a settling region for the test gas to stagnate before it passes through the facility nozzle. Consequently, the nozzle supply pressure, p_0, may be related to the barrel fill pressure, p_b, and the plug valve head loss, H_L, using Eqn (3) as follows:

$$p_0 = p_b - H_L \tag{3}$$

$$\frac{dp_0}{dt} = \frac{dp_b}{dt} - \frac{dH_L}{dt} \tag{4}$$

Differentiating gives Eqn. 4, from which it can be seen that in order to achieve a steady supply pressure ($\frac{dp_0}{dt} = 0$), then $\frac{dp_b}{dt} = \frac{dH_L}{dt}$, implying that the plug valve opening must be tailored and that the head loss should be a function of the open area.

A schematic x-t wave diagram of a Ludwieg Tunnel operating in PALM, with required valve opening overlaid, is shown in Fig. 4a. To achieve PALM operation, the valve opening must feature two distinct stages. The first, occurring between time zero and t_{wr}: the *partial opening* of the valve. The valve opening at the end of this stage governs the supply pressure of the plateau, with greater opening leading to higher supply pressures. The second stage tailors the remaining valve opening to produce a plateau. The steadiness of the plateau is determined by the speed of valve opening in the second stage. If the valve opening is too fast, $\frac{dp_b}{dt} < \frac{dH_L}{dt}$ and the supply pressure decreases (see Fig. 4b). Conversely, if the valve opening is too slow, $\frac{dp_b}{dt} > \frac{dH_L}{dt}$ and the supply

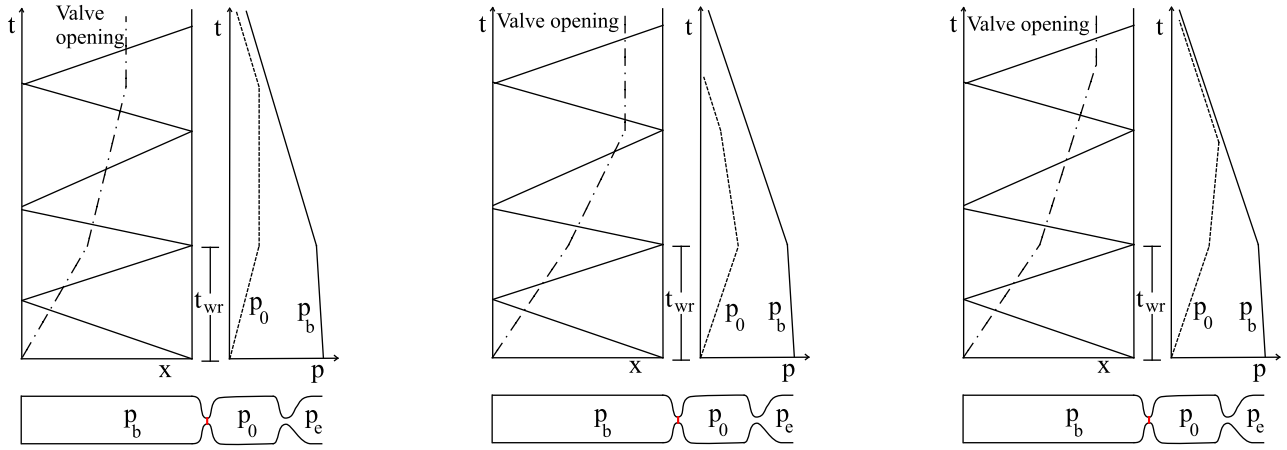

(a) Tailored PALM (b) Second stage motion too fast c) Second stage motion too slow

Fig. 4: Schematic x-t and p-t diagrams showing the effect of different valve openings on the resultant PALM supply pressure trace trace. The red line in the schematics indicates the location of the fast acting valve

pressure increases (see Fig. 4c). In both cases, once the valve has fully opened, the head loss can no longer be tailored and the supply pressure will follow the barrel pressure trace.

3. OXFORD HIGH DENSITY TUNNEL

The Oxford High Density Tunnel (HDT) is a Ludwieg tunnel located at the Oxford Thermofluids Institute, University of Oxford [14]. A schematic of the facility is given in Fig. 5, featuring a barrel of internal diameter 152 mm and length 17.35 m. The barrel is separated from the nozzle plenum by an upstream facing plug valve. The HDT features four nozzles, each with an exit diameter of approximately 350 mm, covering the range of Mach 4 to Mach 7. The facility barrel can be heated to 550 K, and has a maximum pressure rating of 275 bar. All experiments and simulations presented in this paper were carried out with with the Mach 7 nozzle fitted at a barrel fill pressure of 14 bar and fill temperature of 500 K.

3.1. Plug Valve

The HDT plug valve consists of a piston in a piston housing. A schematic of the plug valve and associated pipework is shown in Fig. 6. The piston is pneumatically actuated, with opening and closing of the valve achieved by depressurising and re-pressurising the piston volume respectively. Depressurisation of the piston volume is achieved by closing V13 and opening V12. The differential pressure acting on the piston increases as the piston volume vents to atmosphere, eventually resulting in the piston displacing downstream, exposing radial slots in the piston housing (henceforth referred to as gas slots). Exposure of the gas slots allows test gas to flow through the valve. Re-pressurisation of the piston volume is achieved by closing V12 and opening V13, causing the piston to move forward and cover the gas slots, thereby re-sealing the barrel from the nozzle plenum. The plenum is sealed from the piston volume by circumferential seals on the piston body, and isolated from the barrel by a copper sealing ring acting on the conical face of the piston.

For the HDT, the maximum area through the gas slots is greater than the area of the plug valve throat. Consequently, for operation of the HDT in ELM/PALM, there are three important piston positions:

1. x_1: The exposed area of the gas slots is equal to the area of the plug valve throat, $\mathrm{A_{th}}$.
2. x_2: Gas slots are fully exposed
3. x_{wr}: Piston displacement at t_{wr}

When the piston is at x_1, the flow no longer sees a restriction from the piston. Thus, for HDT, the plug valve being *fully open* is defined as the piston being at position x_1, with ELM being implemented if $x_{wr} \leq x_1$. Smaller values of x_{wr} correspond to the case where $t_{op} > t_{wr}$ discussed in Section 2, with smaller values of x_{wr} resulting in lower peak supply pressures. Subsequent displacement of the piston between x_1 and x_2 allows for the head loss to continue to be tailored after the plug valve is *fully open*, extending the maximum length of the plateau that can be attained in the HDT when operating in PALM.

3.2. Implementation of new modes in the HDT

For ELM, slowing of the plug valve opening was achieved via the install of an orifice downstream of V12, thereby restricting the mass flow through the vent line and reducing the resultant piston speed. The orifice size was sized assuming

steady choked mass flow rate, with no losses in the pipework, using Eqns (5) and (6).

$$\Delta m_{pv} = \frac{p_{pv} A_p x_1}{R T_{pv}} \quad (5) \qquad \dot{m}_{pv} = \frac{\Delta m_{pv}}{t_{wr}} \quad (6)$$

Where Δm_{pv} is the mass of air that must be displaced from behind the piston, p_{pv} is the pressure of the gas behind the plug valve, A_p is the cross-sectional area of the piston, x_1 is the piston displacement for the area in the gas slots to be equal to that of the plug valve throat, R is the specific gas constant of air, T_{pv} is the temperature of the gas behind the plug valve, $\dot{m}_{pv}$ is the required choked mass flow rate through the orifice and t_{wr} is the time it takes for the head of the rarefaction wave to return to the plug valve. For the initial implementation of ELM, a 3.45 mm diameter orifice was used.

PALM requires a two-stage piston motion which was achieved via further modification of the plug valve vent line pipework (replacing the orifice previously installed for ELM). Shown in Fig .6, two manual needle valves and a a pilot operated solenoid valve, PV1, were installed, with the solenoid upstream of one needle valve. For the first stage of motion, PV1 is open, and the gas vents through both needle valves. Closing PV1 reduces the mass flow rate from behind the piston, reducing the rate of change of pressure behind it and providing the slower second stage motion.

3.3. Instrumentation

The facility nozzle supply pressure was measured 265 mm upstream of the nozzle throat using a flush mounted Kulite XCQ-080 pressure transducer with a range of 70 bar absolute. This sensor was amplified using a Kulite KSC-2 signal conditioner.

The Pitot rake used in these experiments utilised pitot probes, instrumented with Kulite pressure transducers and aspirated thermocouples, to characterise the test flow. The aspirated thermocouples were used to measure the total temperature of the flow, using the data reduction technique described in [15]. The Kulites and thermocouples on the rake were amplified using Flyde FE-H379-TA and Fylde FE-351-UA amplifiers respectively.

All data was recorded using NI PXIe-6368 cards housed in a NI PXIE-1082 chassis. The sensors were recorded at a frequency of 2 MHz during the LM and ELM testing, and at a frequency of 20 kHz during PALM testing. The discrepancy in sampling rate is a result of the high sampling rates required for the pitot rake campaign that ELM testing was part of, and due to the extended recording period required to tune in PALM operation.

4. NUMERICAL STUDIES

To gain further insight into the effect of plug valve opening time on the resultant supply pressure trace, simulations of the HDT were performed using the L1D CFD code [16, 17]. L1D is a quasi-one dimensional Lagrangian flow solver used extensively in the design and modelling of hypersonic impulse facilities (e.g. shock tubes and Ludwieg tubes) where the changes in flow properties are only significant in one dimension [18, 19].

4.1. Geometry

The simulation geometry used in this work is shown in Fig 7. Due to the Lagrangian formulation of the code, L1D requires a relatively smooth variation in geometry between sections of differing diameters. Consequently, it is not possible to simultaneously match the volume, length and area distribution of the facility. For these simulations, the volumes and cross-sectional areas of the facility were preserved, whilst the length was not exactly matched. Choosing to match the volumes and areas allows for the expansions through the facility to be properly modelled [20]. However, an exception was made for the volume around the piston housing, for which the maximum gas slot area was used. The maximum gas slot area is larger than both the equivalent area of the annular volume and the area of the plug valve throat. Using the maximum gas slot area for the volume around the piston housing enabled the full piston displacement to be modelled.

The simulation approximates the plug valve as two valves: the first is located at the plug valve throat, the second is at the maximum area of the gas slots. In the simulation, both valves are opened simultaneously with the same transient area variation. The downstream valve continues to open after the upstream valve is fully open. The use of two valves enabled the motion of the plug valve and the expansion of the barrel gas through the plug valve throat to be modelled. Using a single valve located at the plug valve throat only allows for the piston motion up to x_1 to be modelled. Similarly, a single valve located a the gas slots does not appropriately capture the expansion of the high pressure barrel gas through the plug valve throat in the initial stages of opening.

4.2. Tuning

The L1D model of the facility was tuned to match experimentally measured nozzle supply pressure and temperature traces (measured at the history point in Fig. 7).

Tuning of the facility supply pressure was achieved by the addition of a head loss patch across the facility plug valve to represent the change in flow direction as the flow passes through the valve. The remainder of the facility barrel was modelled as inviscid, which allowed for the pressure drop caused by the rarefaction wave to be better matched.

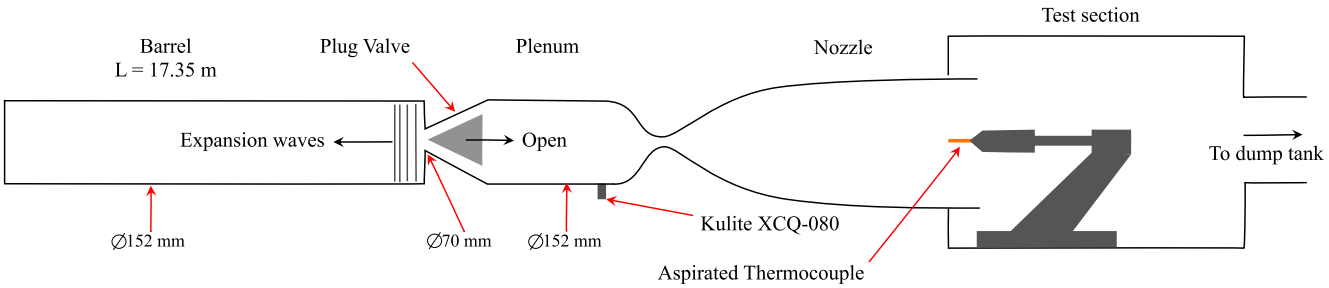

Fig. 5: Schematic of the Oxford High Density Tunnel with a pitot rake installed. The indicated Kulite and aspirated thermocouple provide measurements of the facility supply pressure and total temperature respectively. Reproduced from [15]

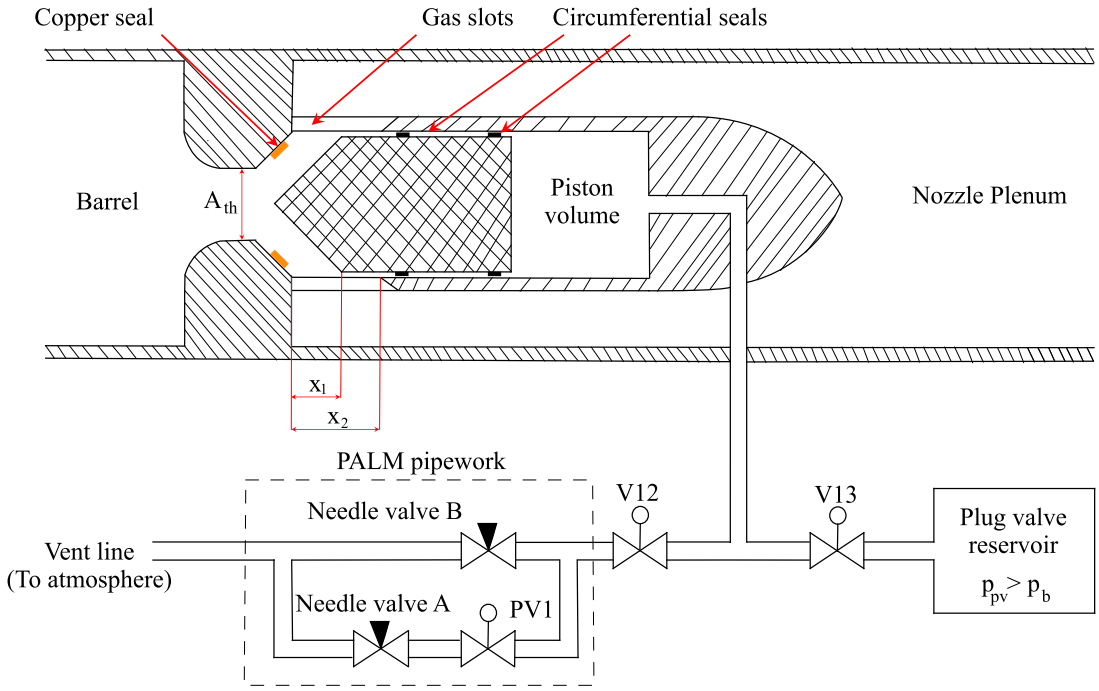

Fig. 6: Schematic of the HDT plug valve at displacement x_1 with the PALM pipework installed

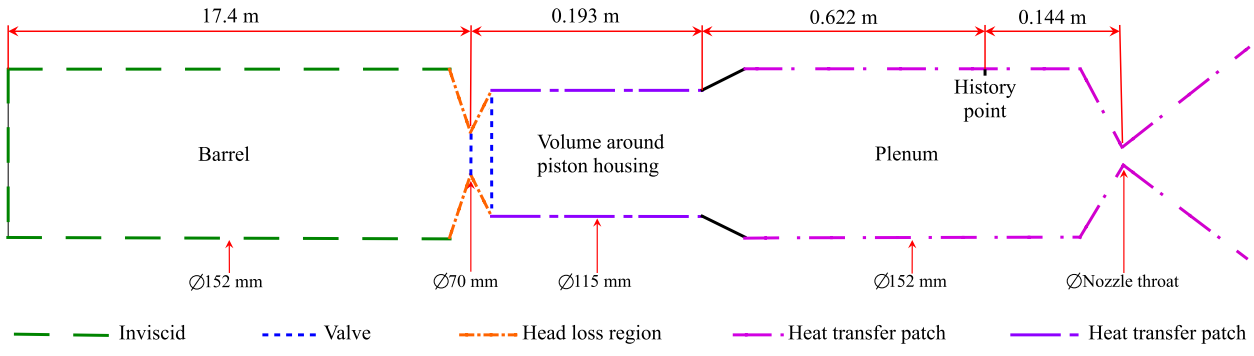

Fig. 7: Representation of the L1D HDT geometry

Total temperature tuning requires an accurate wall temperature along the length of the facility. The HDT features insulated heaters between the rear face of the barrel and upstream face of the plenum, so the temperature of this region was set to the fill temperature. Downstream of the heaters, the facility plenum and nozzle are uninsulated, and so the wall temperature was defined by a series of temperature patches, based on measurements of the plenum walls taken with a barrel fill temperature of 500 K. The total temperature was then tuned by a combination of two heat transfer patches, in which the local heat transfer co-efficient between the gas slug and the wall is increased. This allows modelling of a geometry where the cross-sectional area is not accurately modelled by a tube. The first patch was added to the volume around the piston housing, where the flow passes through an annular area. The second heat transfer patch was located across the facility plenum, where the heat transfer coefficient was increased to account for the large temperature gradient.

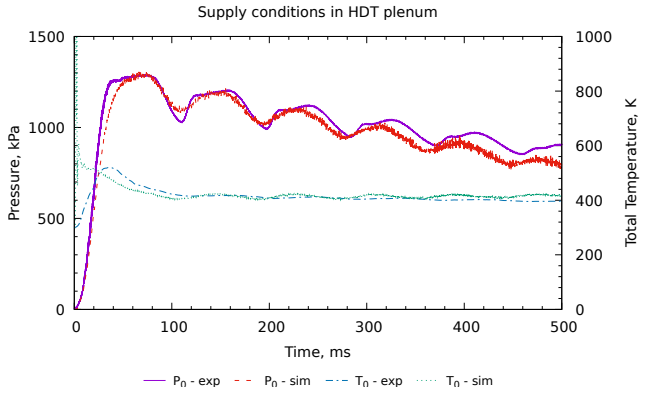

Fig. 8: Comparison between experimental and simulated HDT Supply conditions at the tuned barrel fill conditions of 14 bar, 500K.

The results of this tuning are shown in Fig. 8, from which it can be seen that the tuned L1D model closely matches the experimental nozzle supply pressure trace. There are two main discrepancies between the simulation and experimental data. The first is in the wave timings of the facility, in which the simulated arrival of the reflected head of the rarefaction wave precedes the experimental case. This a consequence of the L1D geometry not matching the physical length of the facility. This discrepancy becomes more apparent at later times (t $>$ 240 ms), as the rarefaction wave reflects and the speed of sound in the barrel decreases. The second discrepancy is in the magnitude of pressure drop between plateaus, which is smaller in the simulation relative to experimental data. This is a result of the head loss tuning across the plug valve, and is most evident at the end of the first plateau. The tuned model also closely matches the experimental total temperature trace, accurately predicting the steady state total temperature, with a slight over-prediction on the last two plateaus.

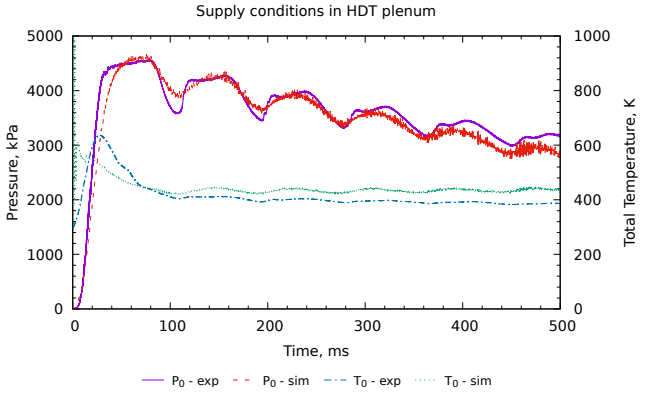

Fig. 9: Comparison between experimental and simulated HDT Supply conditions at 50 bar, 500K

This tuning was compared against another Mach 7 test with fill conditions of 50 bar, 500 K. The results are shown in Fig. 9. As expected, the supply pressure from the tuned simulation accurately predicts the experimental trace. However, it can be seen that the total temperature tuning is not as robust - there is a greater offset between simulated and experimental steady state total temperature, and the transient increase in total temperature at the start of the shot is less well matched.

Overall, the tuned L1D model was found to accurately predict the supply pressure attained in a Mach 7 Ludwieg Mode shot, independent of facility fill pressure. In comparison, it was found that the total temperature tuning is more dependent on the initial fill conditions. Future work may include development of a tuning map of the facility, consisting of the required tuned heat transfer patches for each Mach number, fill pressure and fill temperature. Noting that all further simulations will be conducted at the tuned fill condition, it was decided that the L1D model was sufficiently accurate to predict the performance of the HDT in the new modes.

4.3. Numerical results

The tuned L1D model was then used to investigate the effects of different valve opening times on supply pressure and total temperature. The results are shown in Fig. 10 and Fig. 11 for four cases: 1) Simulated Ludwieg Mode, $t_{op} = 30$ms 2) ELM, $t_{op} = 85$ ms, 3) High Pressure (HP) PALM, $x_{wr} = 0.85x_1$ and $t_{op} = 325$ms, and 4) Low Pressure (LP) PALM, $x_{wr} = 0.5x_1$ and $t_{op} = 2500$ms. It can be seen that L1D confirms both new modes of operation, predicting a steady decrease in supply pressure for ELM and a steady supply pressure of 80% LM peak supply pressure for approximately 200 ms for the HP PALM case. It can be seen that the simulated supply pressure for the LP PALM case exhibits a steady increase in supply pressure, corresponding to Fig. 4c in Sec 2.2. Further work will include increasing t_{op} in this simulation until the required valve opening for tailored PALM is attained. However, it can be seen that increasing the value of x_{wr} dur-

ing PALM operation results in a plateau that is both higher in pressure and shorter in duration. For the HP PALM case, after the plateau is over, the supply pressure decreases at the same rate as ELM.

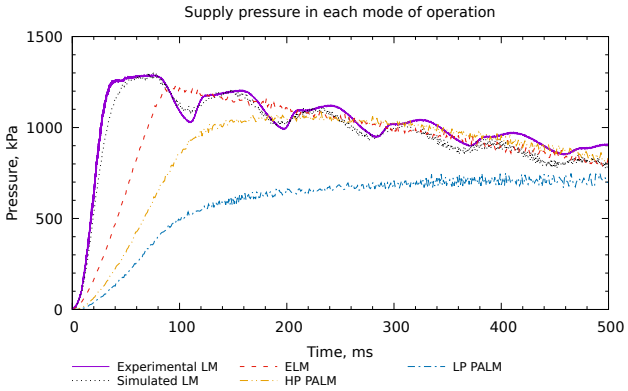

Fig. 10: Comparison between L1D predicted supply pressure traces across the 3 modes of operation of HDT with a fill conditions of 14 bar, 500 K.

The results for the L1D predicted total temperature in each mode of operation are shown in Fig. 11. It can be seen that the predicted total temperature in all modes is consistent for $t > 180$ ms. However, L1D predicts a significant decrease in the magnitude of the transient increase in total temperature a the beginning of a test when HDT is operated in ELM and PALM. This is to be expected as the transient increase in LM is a result of rapid, unsteady filling of the facility plenum. In ELM and PALM, this process occurs over a longer time and so the transient increase is smaller in magnitude.

These L1D simulations have served to confirm the potential of ELM and PALM for enabling longer test time experiments in Ludwieg Tunnels.

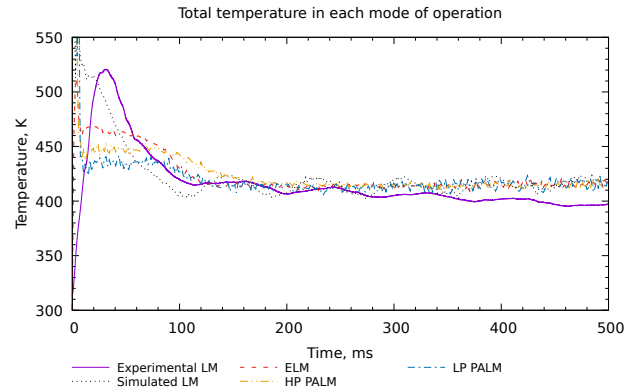

Fig. 11: Comparison between L1D predicted total temperature traces across the 3 modes of operation of HDT with a fill conditions of 14 bar, 500 K.

5. EXPERIMENTAL RESULTS

This section presents results from a test performed in each mode of the HDT: LM, ELM and PALM. Fig 12 presents experimental traces for the measured nozzle supply pressure, freestream total temperature and inferred unit Reynolds number. Also provided are the calculated rates of change. The LM trace in Fig. 12a exhibits an increase in supply pressure after every return of the rarefaction wave. This is a consequence of the diameter of the Mach 7 nozzle throat being approximately 55% smaller than the diameter of the plug valve throat. Additionally, it can be seen from Fig. 12a that the facility begins to shut down at approximately t = 520 ms in Ludwieg Mode. For clarity, the LM data in all subsequent plots is therefore truncated at t = 500 ms. The ELM trace in Fig. 12a shows a steady decrease in supply pressure has been attained for approximately 500 ms. By comparing the location of the peak supply pressure in ELM to the end of the first plateau on the LM trace, it can be seen that the opening of the plug valve was slower than required for ELM. As discussed in section 2.1, this reduces the peak supply pressure attained (for a given fill pressure), but does not impede the resultant steady decrease in pressure. The supply pressure results obtained in PALM exhibit a similar rise time to the ELM trace, but the peak supply pressure attained is lower; a consequence of the lower value of x_{wr} required for PALM. This initial implementation of PALM has resulted in a steady decrease in supply pressure for approximately 300 ms, but at a significantly reduced rate relative to ELM. As discussed in Section 2.2, this decrease in supply pressure indicates that the piston motion during the second stage of opening was too slow and that the effective diameter of needle valve B was too great. The test time achieved in PALM was limited in the current implementation by the reduced mass flow behind the piston. The slower motion of the piston ultimately resulted in the piston changing its direction of motion, prematurely ending the test flow. Subsequent testing at Mach 6 has shown that a secondary actuation of PV1 alleviates this issue, resulting in a test time of approximately 700 ms. As this data is not part of a consistent data set, it is not presented in this paper.

A comparison between the total temperatures is given in Fig. 12b. In all three modes, there is a transient increase in the total temperature at the start of the test due to the unsteady filling of the nozzle plenum. It can be seen that this transient increase is both larger in magnitude and longer in ELM than in LM, whereas for PALM the magnitude is smaller, but with a duration consistent with ELM. In all cases, the total temperature is consistent for t $>$ 200 ms, which corresponds to the 3rd plateau of the LM trace.

Fig 12c presents the variation in unit Reynolds number, calculated assuming perfect gas and isentropic expansion through the facility nozzle, using Keyes' model for viscosity. The unit Reynolds number traces follow the supply pressure traces, with LM producing short plateaus and ELM and

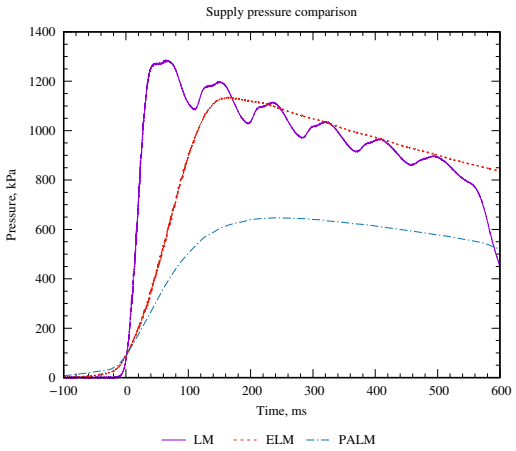

(a) Supply pressure traces

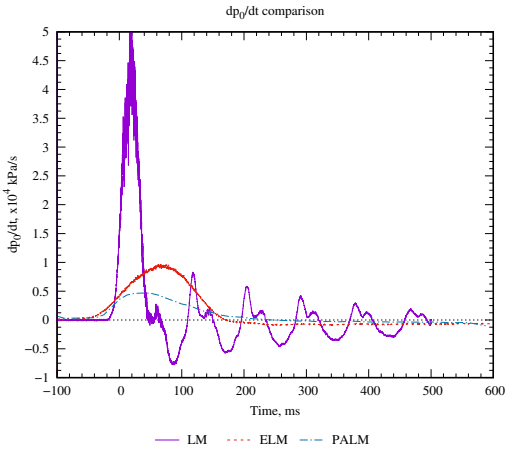

(d) Rate of change of supply pressure

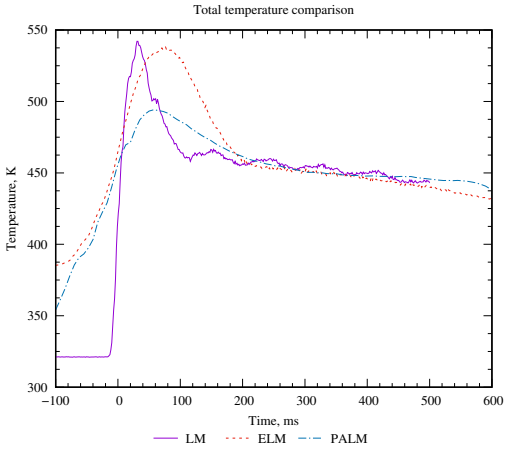

(b) Total temperature traces

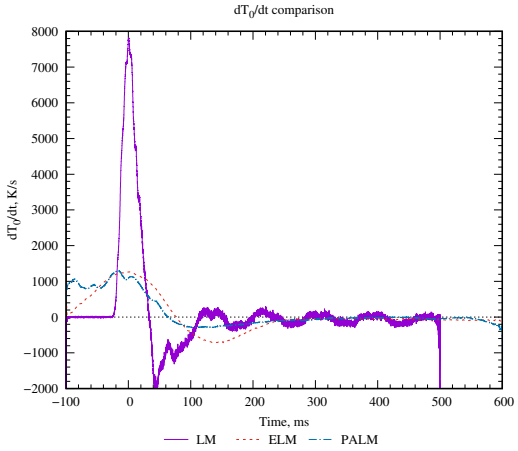

(e) Rate of change of freestream total temperature

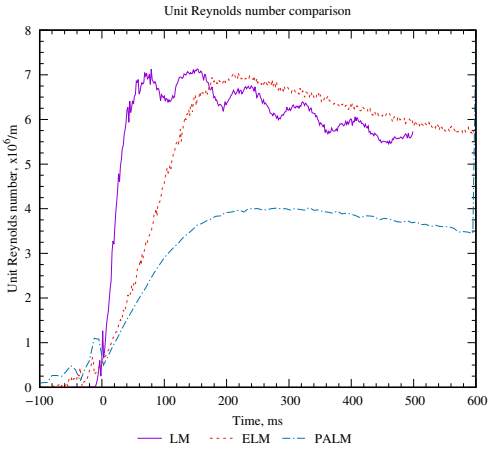

(c) Unit Reynolds number traces

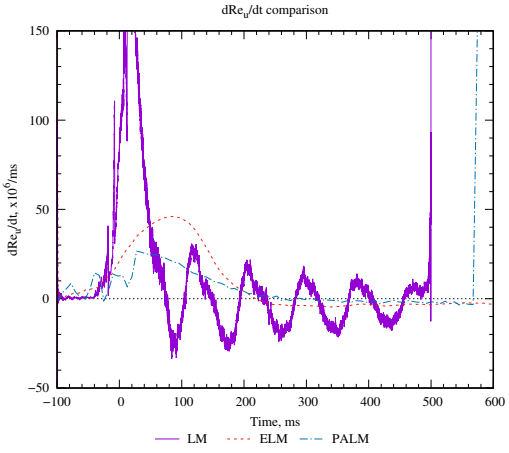

(f) Rate of change of unit Reynolds number

Fig. 12: Comparisons between LM, ELM and PALM. The x axis is also displayed on the local derivative traces, representing the steady case

Table 1: Table comparing the steadiness of the 3 different modes. All values for LM have been averaged on the second plateau

Mode	$\lvert\frac{dp_0}{dt}\rvert$, $\mathrm{kPa\,s^{-1}}$	$\lvert\frac{dT_0}{dt}\rvert$ $\mathrm{K\,s^{-1}}$	$\lvert\frac{dRe_u}{dt}\rvert$, $\mathrm{x10^6\ s^{-1}\,m^{-1}}$	Test Time
LM	859	62.5	6.35	30
ELM	733	58.1	3.49	500
PALM	340	48	1.53	300

PALM resulting in a steady decrease in unit Reynolds number for extended periods of time.

As discussed in Section 1, the steadiness of the test flow is determined by the magnitude of the local derivative of flow properties. Figs. 12d, 12e, and 12f thus present the local derivatives of supply pressure, total temperature and unit Reynolds number, respectively. For all properties, it can be seen that the local derivatives in LM exhibit a large initial transient increase before decaying and oscillating about zero. For a Ludwieg Tunnel operating in LM, the local derivatives would be expected to be zero across a plateau, but it can be seen this is not the case for the HDT operating at Mach 7. These non-zero local derivatives are again a consequence of the small diameter of the Mach 7 nozzle throat relative to the plug valve throat. Operation in ELM and PALM results in a lower initial transient increase in the local derivatives, before decaying to an approximately steady state for $\mathrm{t} > 250\ \mathrm{ms}$.

Table 1 provides a comparison between the average local derivatives over the test time in each of the modes, with LM data being averaged on the second plateau. It can be seen that ELM produces a test flow that is of comparable steadiness in supply pressure and total temperature to a LM plateau, but for a duration that is over 15 times longer. Additionally, operation in ELM presents a significant improvement to the steadiness of the Unit Reynolds number relative to LM, decreasing the magnitude of the local derivate by approximately 45%. Similarly, this initial implementation of PALM has resulted in a test time that is both 10 times longer and significantly steadier than a LM plateau, decreasing the magnitude of local derivative by 60% for supply pressure and 75% for unit Reynolds number, despite the plug valve motion in the second stage being faster than required. It is expected that future implementations of PALM will be able to build on this improvement, and provide extended, steady test times.

6. CONCLUSION

This paper has presented theoretical, numerical and experimental experimental results from the implementation of two new modes of operation for Ludwieg Tunnels that feature an upstream plenum and fast-acting valve. These new modes, Extended Ludwieg Mode (ELM) and Plenum Augmented Ludwieg Mode (PALM) both provide an increased test time compared with Ludwieg Mode, albeit at reduced Reynolds number capability. Both modes have been implemented in the Oxford High Density Tunnel. Operation in ELM has resulted in a test flow that is over fifteen times longer than, but of comparable steadiness to, a Ludwieg Mode plateau in the Oxford High Density Tunnel. PALM was implemented with partial success, resulting in a test flow that is both ten times the duration of, and significantly steadier (for supply pressure and unit Reynolds number), than a Ludwieg Mode plateau. The results demonstrate the potential of PALM for achieving steady test times of extended durations in Ludwieg Tunnels. It is expected that future implementations of PALM in the Oxford HDT will achieve steady test flows with durations in excess of 500 ms. Thus, both ELM and PALM significantly expand the capability of Ludwieg Tunnels for studying long duration flow phenomena such as wake flows, control of hypersonic vehicles and fluid-structure interactions. However, ELM and PALM both also exhibit an increase in the start-up period of the facility, potentially making these modes of operation unsuitable for certain types of experiments (e.g. free-flight [21, 22, 23]). Additionally, operation in PALM results in a decrease in the peak supply pressure that can be attained for a given fill pressure compared to Ludwieg Mode, significantly reducing the unit Reynolds number capability of PALM. Noting that the Oxford HDT is rated for a maximum fill pressure of 275 bar [10, 14], it is expected that nozzle supply pressures of over 60 bar will be attainable in PALM, which covers the range of LM tests conducted to date in this facility.

Future work will include a refinement of pipework and numerical models to enable PALM to be better understood and implemented in the HDT.

Acknowledgements

Many thanks are given to Mailys Buquet for her operation of the HDT during the ELM campaign, Maxime Dahmani Moussa for his operation during the PALM campaign and to Orin Varley for his help in performing the initial PALM testing. Thanks also to Hal Surtell and William Godfrey for assembly and install of the PALM pipework.

7. REFERENCES

[1] Steven P Schneider, "Flight data for boundary-layer transition at hypersonic and supersonic speeds," *Journal of Spacecraft and Rockets*, vol. 36, no. 1, pp. 8–20, 1999.

[2] Shelly Ferlemann, Charles McClinton, Ken Rock, and Randy Voland, "Hyper-x mach 7 scramjet design, ground test and flight results," in *AIAA/CIRA 13th International Space Planes and Hypersonics Systems and Technologies Conference*, 2005, p. 3322.

[3] Timothy Wadhams, Matthew MacLean, Michael Holden, and Scott Barry, "A review of transition studies on full-scale flight vehicles at duplicated flight conditions in the lens tunnels and comparisons with prediction methods and flight measurement," in *48th AIAA Aerospace Sciences Meeting Including the New Horizons Forum and Aerospace Exposition*, 2010, p. 1246.

[4] C Cockre, A Auslender, J White, and A Dilley, "Aeroheating predictions for the x-43 hyper-x cowl-closed configuration at mach 7 and 10," in *40th AIAA Aerospace Sciences Meeting & Exhibit*, 2002, p. 218.

[5] Sangdi Gu and Herbert Olivier, "Capabilities and limitations of existing hypersonic facilities," *Progress in Aerospace Sciences*, vol. 113, pp. 100607, 2020.

[6] Frank K Lu and Dan E Marren, "Principles of hypersonic test facility development," *Progress in Astronautics and Aeronautics. Volume 198*, pp. 17–27, 2002.

[7] RJ Stalker, "Modern developments in hypersonic wind tunnels," *The Aeronautical Journal*, vol. 110, no. 1103, pp. 21–39, 2006.

[8] Matthew McGilvray, Rainer Kirchhartz, and Thomas Jazra, "Comparison of mach 10 scramjet measurements from different impulse facilities," *AIAA journal*, vol. 48, no. 8, pp. 1647–1651, 2010.

[9] Matthew McGilvray, Richard G Morgan, and Peter A Jacobs, "Scramjet experiments in an expansion tunnel: evaluated using a quasi-steady analysis technique," *AIAA journal*, vol. 48, no. 8, pp. 1635–1646, 2010.

[10] Sebastien Wylie, Luke Doherty, and Matthew McGilvray, "Commissioning of the oxford high density tunnel (hdt) for boundary layer instability measurements at mach 7," in *2018 Fluid Dynamics Conference*, 2018, p. 3074.

[11] Aaron T Dufrene, "Extension of lens shock tunnel test times and lower mach number capability," in *53rd AIAA Aerospace Sciences Meeting*, 2015, p. 2017.

[12] TV Jones, P Street, and M Westby, "Recent enhancements to the dra shock tunnel," *Wind tunnels and wind tunnel test techniques*, p. 30, 1992.

[13] Roger L Kimmel, Matthew P Borg, Joseph S Jewell, KIng-Yiu Lam, Rodney D Bowersox, Ravi Srinivasan, Steven Fuchs, and Thomas Mooney, "Afrl ludwieg tube initial performance," in *55th AIAA Aerospace Sciences Meeting*, 2017, p. 0102.

[14] Matthew McGilvray, Luke J Doherty, Andrew J Neely, Robert Pearce, and Peter Ireland, "The oxford high density tunnel," in *20th AIAA International Space Planes and Hypersonic Systems and Technologies Conference*, 2015, p. 3548.

[15] McGilvray M Hambidge C Herman T. and Buttsworth D., "Total Temperature Measurements In the Oxford High Density Tunnel," *FAR Conference, Monopoli, Italy*, 2019.

[16] PA Jacobs, "Quasi-one-dimensional modeling of a free-piston shock tunnel," *AIAA journal*, vol. 32, no. 1, pp. 137–145, 1994.

[17] Peter A Jacobs, "Shock tube modelling with l1d," 1998.

[18] Peter L Collen, Luke Doherty, Matthew McGilvray, Imran Naved, Rowland T Penty Geraets, Tobias A Hermann, Richard G Morgan, and David Gildfind, "Commissioning of the t6 stalker tunnel," in *AIAA Scitech 2019 Forum*, 2019, p. 1941.

[19] Peter Collen, Luke J Doherty, Suria D Subiah, Tamara Sopek, Ingo Jahn, David Gildfind, Rowland Penty Geraets, Rowan Gollan, Christopher Hambidge, Richard Morgan, et al., "Development and commissioning of the t6 stalker tunnel," *Experiments in Fluids*, vol. 62, no. 11, pp. 1–24, 2021.

[20] Andreas Andrianatos, "Ground testing at superorbital flight conditions in a large scale expansion tube," 2020.

[21] Andrew Hyslop, Luke J Doherty, Matthew McGilvray, Andrew Neely, Liam P McQuellin, James Barth, and Gerrie Mullen, "Free-flight aerodynamic testing of the skylon space plane," *Journal of Spacecraft and Rockets*, vol. 58, no. 5, pp. 1487–1497, 2021.

[22] Andrew M Hyslop, Matthew McGilvray, and Luke J Doherty, "Free-flight aerodynamic testing of a 7 degree half-angle cone," in *AIAA SCITECH 2022 Forum*, 2022, p. 1324.

[23] Liam P McQuellin, Christopher M Kennell, Joni M Sytsma, Rishabh Choudhury, Andrew Neely, David R Buttsworth, and Todd Silvester, "Investigating endo-atmospheric separation of a hypersonic flyer-sustainer using wind tunnel based free-flight," in *23rd AIAA International Space Planes and Hypersonic Systems and Technologies Conference*, 2020.